Insight into the radial sensitivity of phenomenological nucleus-nucleus interaction potentials

L. Yang,[1] C. J. Lin,[1,2,*] H. M. Jia,[1] D. X. Wang,[1] N. R. Ma,[1] P. W. Wen,[1] F. Yang,[1] F. P. Zhong,[1,2] S. H. Zhong,[1,2] and T. P. Luo[1]

[1]*China Institute of Atomic Energy, P.O. Box 275(10), Beijing 102413, China*

[2]*Department of Physics, Guangxi Normal University, Guilin 541004, China*

(Received 24 February 2020; accepted 22 April 2020; published 6 May 2020)

The optical model potential, which reflects an overall feature of the nuclear property and reaction dynamics, has been widely adopted to describe the nucleus-nucleus interaction phenomenologically. Experimentally, knowledge of the optical potential can only be learned in the vicinity of a sensitive radius. In this study, the notch technique was applied to extract the radial sensitive regions of the tightly bound system $^{16}O + ^{208}Pb$ and weakly bound systems $^{9}Be + ^{208}Pb$ and $^{6}He + ^{209}Bi$ at energies around the Coulomb barrier. It is the first time that we observed two distinct sensitive regions, corresponding to the inner volume absorption and the outer surface absorption processes. Strong energy dependence of the sensitive regions was found as well. Based on this result, we further investigated the interaction property of $^{9}Be + ^{208}Pb$ and found that the threshold anomaly was observed in the volume interaction, whereas the abnormal near-threshold behavior was presented in the surface part.

DOI: 10.1103/PhysRevC.101.054603

I. INTRODUCTION

The optical model potential (OMP) has been extensively utilized with great success to describe the complicated nucleus-nucleus interaction phenomenologically. The energy dependence of the optical potential reflects the dynamic polarization, which originates from the couplings between different reaction channels. For example, for the systems containing tightly bound nuclei, the phenomenon of threshold anomaly (TA) [1] is presented, which is characterized by the sharp decrease of the imaginary part of the potential as the bombarding energy decreases towards the Coulomb barrier, associated with a localized peak around the barrier in the real part. The dispersion relation [2], which is a natural consequence of the causality principle, connects the real and imaginary potentials. The situation, however, becomes more complicated for the systems involving weakly bound nuclei, such as ^{6}He [3–6], ^{6}Li [7,8], and ^{9}Be [9]. For these systems, the breakup and/or transfer channels may remain largely open at energies below the Coulomb barrier, and a distinct manifestation of the OMP was observed, demonstrated as an increasing trend in the imaginary potential with energy decreasing below the barrier. Furthermore, the applicability of the dispersion relation for these exotic systems is a long-standing puzzle [2,4–6,10–13].

It is well known that all the quantities of OMP are based on the values of the potentials in the vicinity of the sensitive radius, which is established before any substantial overlap of the two nuclear matter distributions [14,15]. It is therefore crucial and necessary to ascertain what radial region of the nuclear potential can be well mapped before we discuss the properties of OMP. One of the frequently used methods to determine the sensitive region (SR) is to find the crossing-point radius of the potential [16,17]. Such a sharply defined sensitive radius, however, is incompatible with the principles of quantum mechanics, and its value varies with the radial form factor adopted for OMP [15]. As an alternative, the notch technique permits an intuitive investigation of the SR and was developed by Cramer *et al.* [18]. The principle of the notch technique is to introduce a localized perturbation into the radial potential and move the notch radially through the potential to investigate the influence arising from this perturbation on the predicted cross section. Taking the real part potential as an example, the perturbation $V_{\rm notch}$ is expressed as

$$V_{\rm notch} = dV_0 f_V(R', a, R_{\rm int}) f_{\rm notch}(r, a', R'). \tag{1}$$

V_0 is the depth of the real potential, $f_V(R', a, R_{\rm int})$ is the Woods-Saxon form with a and $R_{\rm int}$ representing the diffuseness and interaction radius. $R_{\rm int}$ is expressed as $R_{\rm int} = r_0(A_{\rm P}^{1/3} + A_{\rm T}^{1/3})$, where $A_{\rm P}$ and $A_{\rm T}$ denote the mass numbers of the projectile and target, respectively. d is the fraction by which the potential is reduced. $f_{\rm notch}(r, a', R')$ denotes the derivative Woods-Saxon surface form factor, where R' and a' represent the position and width of the notch. In our previous work [19], the sensitivities of the notch technique to the perturbation parameters as well as to the experimental data were investigated in detail. Based on these results, we further applied the notch technique to study the properties of SRs of $^{16}O + ^{208}Pb$ [20–22], $^{9}Be + ^{208}Pb$ [9], and $^{6}He + ^{209}Bi$ [3–6,23,24], which are employed as typical examples of tightly and weakly bound systems as well as halo nuclear systems, respectively.

*Corresponding author: cjlin@ciae.ac.cn

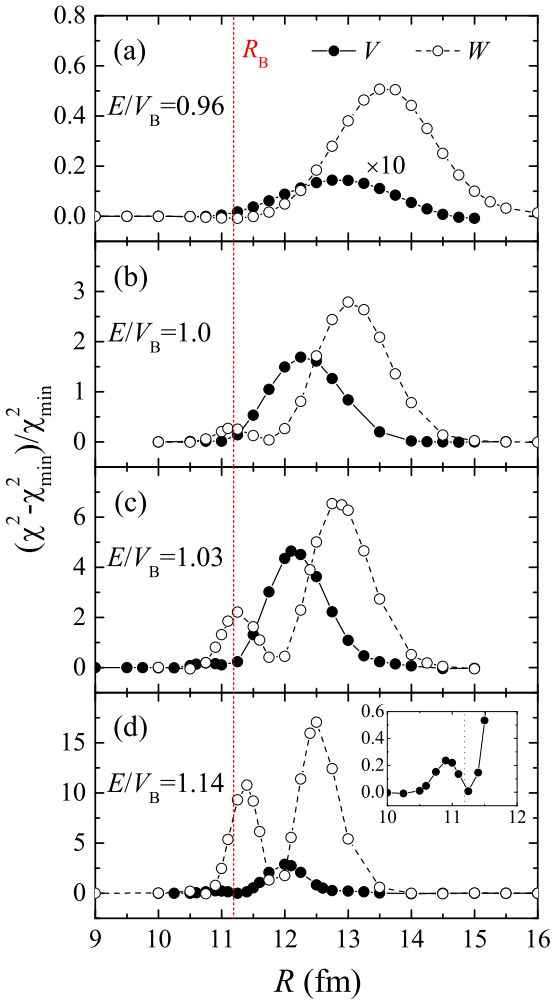

FIG. 1. Sensitivity functions for the real (full circle) and imaginary (hallow circle) potentials for ^{9}Be + ^{208}Pb at some typical energies, with the experimental data taken from Ref. [9]. The vertical dashed curves denote the positions of R_B. The fine structure of the inner SR of the real potential at $E/V_B = 1.14$ is shown in the inset of (d).

II. APPLICATION OF THE NOTCH TECHNIQUE AND DISCUSSION

According to the results reported in Ref. [19], the values of d and a' were fixed at 1.0 and 0.05 fm, respectively. The Woods-Saxon radial form factor was adopted for the nuclear potential. The reduced radius r_0 and the diffuseness parameter a were fixed at 1.25 and 0.65 fm for ^{16}O + ^{208}Pb, 1.24 and 0.63 fm for ^{9}Be + ^{208}Pb. For ^{6}He + ^{209}Bi, $r_0 = 1.02$ fm and $a = 0.70$ fm for the real potential, while, for the imaginary part, $r_0 = 1.25$ fm and $a = 0.95$ fm [4]. The depths of the real and imaginary potentials were then extracted by fitting the elastic scattering angular distributions. All the optical model (OM) calculations in the present work were performed with the code FRESCO [25].

The derived radial sensitivities of ^{9}Be + ^{208}Pb at some typical energies are shown in Fig. 1. As references, we also labeled in the figures the radius of the Coulomb barrier R_B, which is derived by the global Broglia-Winther potential [26]. One can find that the nuclear interior (less than the interaction radius R_{int}, which is about 10 fm), where the two nuclei have begun to overlap appreciably, cannot be probed [18]. With energy decreasing, SR moves toward the outside and becomes broader and broader, demonstrating that the sensitivity of the experimental data to the details of the nuclear potential becomes weaker. That is mainly because of the overwhelming effect of the Coulomb repulsion between the target and the projectile at the lower energies. It can be further confirmed by the variations of the relative χ^2 values, which become larger as the energy increases. The relative χ^2 values also indicate that the data are more sensitive to the imaginary potential. Moreover, compared with the real potential, a larger sensitive radial region is observed for the imaginary potential.

Furthermore, from Fig. 1 one can find that two distinct peaks are presented in both the real and imaginary parts within the above barrier energy region. The amplitude of the inner peak decreases rapidly with the energy going down to the subbarrier, especially for the real part, and it is too small to be recognized at lower energies. The position of the inner peak almost stays fixed, having no obvious dependence on the energy; for the real part, the inner peak lies slightly inside of R_B, while that of the imaginary part locates around R_B. Therefore, the inner peak is expected to be responsible for the process of the volume interaction, i.e., the inner peak of the real potential corresponds to the resonance scattering process, and that of the imaginary part arises from the fusion reaction. With the energy decreasing towards the barrier, the probability of the barrier penetration reduces exponentially, leading to a rapidly damped inner peak. The outer peaks, however, locate away from R_B. Thus they are mainly responsible for the surface interaction, i.e., the direct interaction processes: the shaping scattering for the real part and direct reactions for the imaginary part.

The energy dependence of the center of the radial SR derived by using the Gaussian fitting is shown in Fig. 2, where the error bars denote the width (sigma) of SR. For the neutron-halo system ^{6}He + ^{209}Bi, in addition to the elastic scattering data, the notch technique was also applied to the transfer reaction ^{208}Pb(^{7}Li, ^{6}He) ^{209}Bi [4–6] to extract SR of ^{6}He + ^{209}Bi in the exit channel, as the star symbols displayed in Fig. 2(c). Since it is difficult to recognize the SR of the volume absorption of ^{6}He + ^{209}Bi, only the results of the surface interaction are shown. As a comparison, the strong absorption radius (R_{sa}) and the closest approach of a head-on collision in the Coulomb field D_0 are also presented, as shown by the triangles and solid curves, respectively. R_{sa}, at which the observed elastic scattering cross section has fallen to one-fourth of the Rutherford value, was derived experimentally. It can be seen clearly that, in the above barrier region, the surface interaction (SR_{sur}) locates around R_{sa}. In the sub-barrier region, however, the behavior of SR_{sur} is consistent with D_0, as shown by the solid curve.

For ^{6}He + ^{209}Bi, SR_{sur} of the imaginary potential lies over a larger region than that of D_0 in the sub-barrier region. It illustrates that the absorption of flux from the elastic channel of ^{6}He + ^{209}Bi starts to occur at long distances, as can be expected for a projectile with the halo structure. The inner SR

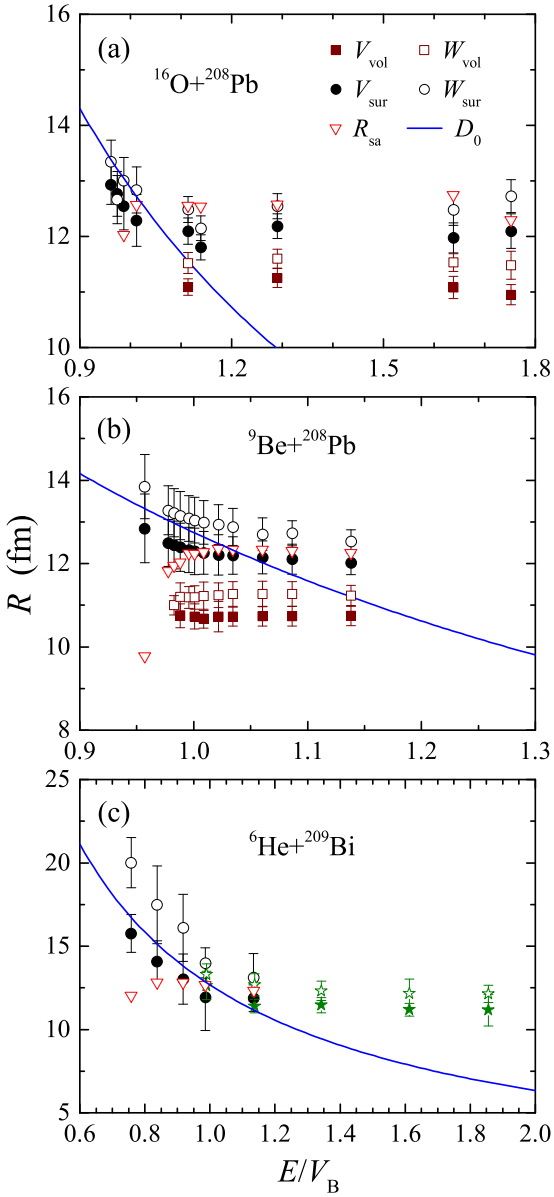

FIG. 2. Energy dependence of SRs for (a) $^{16}\mathrm{O}+^{208}\mathrm{Pb}$, (b) $^{9}\mathrm{Be}+^{208}\mathrm{Pb}$, and (c) $^{6}\mathrm{He}+^{209}\mathrm{Bi}$. The full and hallow circles represent the results of the surface interaction of the real (V_{sur}) and imaginary (W_{sur}) parts, respectively. The corresponding squares denote the volume SRs of the real (V_{vol}) and imaginary (W_{vol}) potentials. The triangles are R_{sa} extracted from the experimental data, and the solid curves represent the theoretical D_0. SRs of $^{6}\mathrm{He}+^{209}\mathrm{Bi}$ extracted from the transfer reactions [4–6] are also shown in (c), represented by the star symbols.

(SR_{vol}), which corresponds to the barrier penetration process, locates around the Coulomb barrier as discussed above.

Since the SR is the basis to study the OMP, we can move a further step to investigate the properties of OMP, especially for the weakly bound nuclear systems. Due to the existence of SR_{sur} and SR_{vol}, the corresponding potentials, i.e., the volume and surface potentials, should be included explicitly in the OMP. In previous studies [12,27,28], the OMPs have been decomposed into the volume and surface parts to describe the

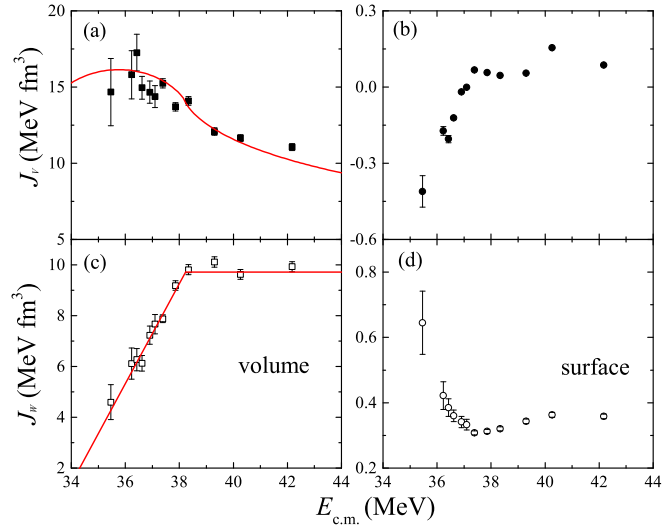

FIG. 3. Energy dependence of the volume integrals of the real (a) and imaginary (c) volume potentials, as well as those [(b) and (d)] of the surface interactions of $^{9}\mathrm{Be}+^{208}\mathrm{Pb}$. The solid curve in (c) shows the linear segment fitting for the imaginary potential. The prediction of the dispersion relation according to the variation of the imaginary potential is presented in (a) by the solid curve.

fusion and elastic scattering data simultaneously. The results of the present work offer direct evidence to support this decomposition approach. To avoid the influence of the variation of the SRs with energy, we used the volume integrals, J, for both the volume and surface interactions, rather than the potential depths at the center of the SR. The outer limit of the SR_{vol} was used as the boundary of the integration interval, to separate the volume and surface regions. The corresponding results of $^{9}\mathrm{Be}+^{208}\mathrm{Pb}$ are shown in Fig. 3, with the OMP parameters taken from Ref. [28]. One can find that the TA phenomenon is presented for the volume interaction, as shown in Figs. 3(a) and 3(c). The dispersion relation can properly describe the connection between the real and imaginary parts, as shown by the solid curve in Fig. 3(a), which is based on the variation of the imaginary potential with the linear schematic model [2]. For the direct interaction shown in Figs. 3(b) and 3(d), however, the abnormal behavior is observed as claimed in the previous work [9]. Compared with the volume interaction, such a peculiar near-threshold behavior naturally associates with the direct reaction mechanisms. Due to the lack of a complete picture of the imaginary potential, i.e., the turning point at which the potential begins to decrease and the threshold energy where the imaginary potential becomes to zero, it is difficult to assess correctly the applicability of the dispersion relation.

III. SUMMARY AND CONCLUSIONS

In summary, the notch technique was applied to study the radial SR of tightly and weakly bound nuclear systems. The origins of the peaks presented in the sensitivity functions were identified qualitatively for the first time: the inner peak arises from the volume absorption process, i.e., the resonant scattering and the fusion reaction, while the outer

peak corresponds to the surface interaction, i.e., the shaping scattering and the direct reaction. Moreover, the volume SR locates around the Coulomb barrier radius since it relates to the barrier penetration process, while for the surface SR strong energy dependence is observed: it varies around R_{sa} at above barrier energies, and coincides with D_0 below the Coulomb barrier. According to the volume integrals of the volume and surface interactions of $^{9}\mathrm{Be} + {}^{208}\mathrm{Pb}$, the typical TA phenomena were observed for the volume part, whereas the surface potentials present the abnormal behavior, which apparently is associated with the complicated direct reaction mechanisms of the exotic nuclear system. The quantities of the nucleus-nucleus interactions can only be derived within a specific sensitive region experimentally. Therefore, it is desirable to further apply the notch technique to investigate the SR in a wide range of unstable nuclei and to obtain a global and universal understanding of the properties of the interaction potentials of the exotic nuclear systems.

ACKNOWLEDGMENTS

This work is supported by the National Key R&D Program of China (Contract No. 2018YFA0404404), the National Natural Science Foundation of China (Grants No. 11635015, No. U1732145, No. 11705285, No. U1867212, No. 11805280, and No. 11961131012), and the Continuous Basic Scientific Research Project (No. WDJC-2019-13).

[1] J. S. Lilley *et al.*, Phys. Lett. B **128**, 153 (1983).
[2] C. Mahaux, H. Ngo, and G. R. Satchler, Nucl. Phys. A **449**, 354 (1986).
[3] A. R. Garcia, J. Lubian, I. Padron, P. R. S. Gomes, T. Lacerda, V. N. Garcia, A. Gomez Camacho, and E. F. Aguilera, Phys. Rev. C **76**, 067603 (2007).
[4] L. Yang, C. J. Lin, H. M. Jia *et al.*, Phys. Rev. C **89**, 044615 (2014).
[5] L. Yang, C. J. Lin, H. M. Jia *et al.*, Phys. Rev. Lett. **119**, 042503 (2017).
[6] L. Yang, C. J. Lin, H. M. Jia *et al.*, Phys. Rev. C **96**, 044615 (2017).
[7] N. Keeley, S. J. Bennett, N. M. Clarke *et al.*, Nucl. Phys. A **571**, 326 (1994).
[8] C. L. Zhang, H. Q. Zhang, C. J. Lin *et al.*, Chin. Phys. Lett. **23**, 1146 (2006).
[9] N. Yu, H. Q. Zhang, H. M. Jia *et al.*, J. Phys. G: Nucl. Part. Phys. **37**, 075108 (2010).
[10] R. Lipperheide and A. K. Schmidt, Nucl. Phys. A **112**, 65 (1968).
[11] A. Pakou, N. Alamanos, A. Lagoyannis *et al.*, Phys. Lett. B **556**, 21 (2003).
[12] F. Tprabi, E. F. Aguilera, O. N. Ghodsi, and A. Gómez-Camacho, Nucl. Phys. A **994**, 121661 (2020).
[13] R. N. Pèrez and J. Lei, Phys. Lett. B **795**, 200 (2019).
[14] M. E. Brandan and G. R. Satchler, Phys. Rep. **285**, 143 (1997).
[15] M. H. Macfarlane and S. C. Pieper, Phys. Lett. B **103**, 169 (1981).
[16] C. J. Lin, J. C. Xu, H. Q. Zhang, Z. H. Liu, F. Yang, and L. X. Lu, Phys. Rev. C **63**, 064606 (2001).
[17] D. Roubos, A. Pakou, N. Alamanos, and K. Rusek, Phys. Rev. C **73**, 051603(R) (2006).
[18] J. G. Cramer and R. M. DeVries, Phys. Rev. C **22**, 91 (1980).
[19] L. Yang, C. J. Lin, H. M. Jia *et al.*, Chin. Phys. C **40**, 056201 (2016).
[20] C. P. Silva, M. A. G. Alvarez, L. C. Chamon *et al.*, Nucl. Phys. A **679**, 287 (2001).
[21] S. C. Pieper, M. H. Macfarlane, D. H. Gloeckner *et al.*, Phys. Rev. C **18**, 180 (1978).
[22] F. Videbaek, R. B. Goldstein, L. Grodzins, and S. G. Steadman, Phys. Rev. C **15**, 954 (1977).
[23] E. F. Aguilera, J. J. Kolata, F. M. Nunes, F. D. Becchetti, P. A. DeYoung, M. Goupell *et al.*, Phys. Rev. Lett. **84**, 5058 (2000).
[24] E. F. Aguilera, J. J. Kolata, F. D. Becchetti *et al.*, Phys. Rev. C **63**, 061603(R) (2001).
[25] I. J. Thompson, Comput. Phys. Rep. **7**, 167 (1988).
[26] R. A. Broglia and A. Winther, *Heavy Ion Reactions: Lecture Notes, The Elementary Processes* (Addison-Wesley, Reading, MA, 1991).
[27] W. Y. So, S. W. Hong, B. T. Kim, and T. Udagawa, Phys. Rev. C **69**, 064606 (2004).
[28] A. Gómez Camacho, N. Yu, H. Q. Zhang, P. R. S. Gomes, H. M. Jia, J. Lubian, and C. J. Lin, Phys. Rev. C **91**, 044610 (2015).